Construction and Building Materials 167 (2018) 846–852

Contents lists available at ScienceDirect

Construction and Building Materials

journal homepage: www.elsevier.com/locate/conbuildmat

On the tolerable limits of granulated recycled material additives to maintain structural integrity

L.M. Clemon *, T.I. Zohdi

Department of Mechanical Engineering, University of California, Berkeley, CA 94720-1740, USA

HIGHLIGHTS

- Provides a tool to aid circular economy pathways for 3D printer waste.
- Added distribution effects to correlated microstructural stress-macrostructural loads.
- Added distributional effects to particle-matrix stress concentration factors.
- Developed method for rapid material property estimates of mixed waste materials.
- Computational method to accelerate mixed-waste recycled material development.

ARTICLE INFO

Article history:
Received 26 November 2017
Received in revised form 15 February 2018
Accepted 15 February 2018

Keywords:
Particles
Composites
Additive manufacturing
Recycling
Phase averages

ABSTRACT

Production and maker spaces are increasingly generating mixed plastic material waste of varying quality from 3-D printers. Industrial interest is growing in embedding granulated recycled particulate material additives into a virgin binding matrix. Examples include the introduction of granulated mixed recycled materials into 3-D printer material, concrete, and pavement. The stress load-sharing between the particulate additive and the binding matrix is an important factor in design and development of these composite materials. With mixed material additives, a designer is interested in the variation of such predicted load-sharing. However, experimental development is costly and time-consuming, thus analytical and semi-analytical estimates are desired for accelerated development. In this work, we expand on previous analytically correlated phase-averaged micro- and macrostructural loading to include variational effects present in mixed recycled material. In addition, model trade-offs are provided to aid designers in quickly selecting application specific mixtures. This framework identifies the stress contributions, and their variation, to reduce product development time and costs, which could greatly accelerate material recycling and reuse for improved infrastructure materials, low-cost 3-D printer filament, and reduced waste towards a more circular economy.

1. Introduction

Many organizations have stated goals of becoming zero-waste entities, namely no material going to landfills-*anywhere* [1–4]. In addition, municipalities are ever more concerned with odor pollution and potential seepage from landfills within their borders. Strategies have emerged to combat the disposal of plastic waste, in particular [5,6]. Instead, plastic waste products may be processed with automated collection, cleaning, sorting, and grinding for reuse and recycling. Such processes can downcycle the waste into products with less stringent purity requirements than the original. Or, with sufficient sorting and processing, waste may be recycled into the original product [7]. These efforts facilitate a more circular economy. In particular, two target end products are of interest for re- and downcycling nearly all plastics:

1. 3-D printer filament for educational demonstrations and prototypes
2. filler for bulk construction materials, such as construction materials

Education at virtually all levels and in many fields of study have undergone massive changes due to the rise of inexpensive 3-D printers. Unfortunately, the price of 3-D printer material over time is not trivial. In educational and early design environments, the printed material is used primarily to develop form and fit prototypes, which need not be made of high-grade materials. Thus,

* Corresponding author.
E-mail addresses: mclemon@berkeley.edu (L.M. Clemon), zohdi@me.berkeley.edu (T.I. Zohdi).

https://doi.org/10.1016/j.conbuildmat.2018.02.099
0950-0618/

we provide a design framework with example calculations which will aid in determining the maximum extent to which plastic waste may be processed into 3-D printer feedstock and bulk construction material filler. Materials unsuitable for 3-D printer filament may be used in bulk construction materials as a filler thereby closing the loop on the full set of plastic waste. In urban areas with high waste generation and infrastructure needs, the colocation of waste generators and reprocessing facilities would be advantageous for minimizing transportation costs as well. The design methodology in this manuscript may be used to determine mixtures of such particulate materials with existing types of pavement and roadway materials to create near zero-waste materials to maintain and rebuild roadway infrastructure.

Regardless of the final use of the materials, they can be compacted and/or packaged efficiently through grinding and shredding. Collocating the product use with recycling and fabrication would also minimize transportation impact and contribute to local economies. In addition to the obvious reasons for grinding, such as volume-reduction and homogenization, others include secure disposal of potentially sensitive information on electronic devices and storage units. It is particularly important to recognize regulations that are moving towards the responsible reduction and handling of waste to reduce an enterprise's carbon footprint. Granulated waste products can be sold to other enterprises or recycled within the community as filler, pavement, insulation, or other building materials, such as resin-combined briquettes and composite wood products.

It is now commonplace for plastic pellets to be sold as feedstock to a converter for fabrication into consumer products or recycled by hobbyists for individual use. This framework serves to aid designers in diverting more waste from landfills by estimating the composite strength of recycled and virgin material. Thereby enabling rapid development of product streams for recycled waste. Moreover, the statistical variation in such estimates for mixed waste recycling is included for broad applicability.

2. Methodology framework

Industrial interest is growing in particulate-enhanced composite materials for structural applications (Fig. 1). Similarly, many particle-matrix choices available to designers and analysts. Limited experimental success has shown recycled materials may be used in concrete and cement [8,9]. However, such experimental development is expensive and time-consuming for such applications. Thus, characterizing these materials computationally may significantly reduce development time and cost.

Similarly, municipal governments are increasingly concerned over waste quantities and pathways to recycling. The rise of additive manufacturing and 3D printing in classroom, art, hobby, and production environments provides both a source of increased plastic waste and a potential recycling pathway. The use of lower grade materials in prototypes, art, and education is acceptable due to lower strength and durability requirements; some industrial applications may also prefer some quantity of recycled content. The large portion of input material into additive manufacturing that emerges as waste has a distribution of quality ranging from that equivalent to pristine material to some which must be downcycled or disposed of (Fig. 2). As a result, much of the "used", or previously processed, material may be directly inserted into new products. However, the distribution of quality is specific to each additive manufacturing process and machine. The methodology described in this manuscript is broadly applicable to all processing methods given the relevant data.

For a simple mixture of known specific particles mixed into a binding matrix, the effective macroscale (structural) material response seeks a relationship, $\langle \boldsymbol{\sigma} \rangle_{\Omega} = \boldsymbol{IE}^{*} : \langle \boldsymbol{\epsilon} \rangle_{\Omega}$, where

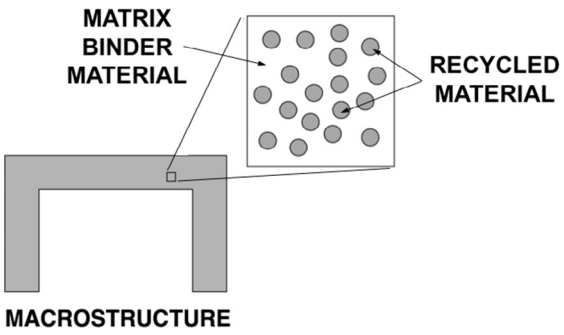

Fig. 1. Example structure with a matrix binder and recycled particulate additives.

$\langle \cdot \rangle_{\Omega} \stackrel{\text{def}}{=} \frac{1}{|\Omega|} \int_{\Omega} \cdot \, d\Omega$,and where the mechanical properties of micro-heterogeneous materials in the structure are characterized by an elasticity tensor $\boldsymbol{IE} = \boldsymbol{IE}(\boldsymbol{x})$ varying in space, with $\boldsymbol{\sigma}$ and $\boldsymbol{\epsilon}$ as stress and strain tensor fields within a Representative Volume Element (RVE) of volume $|\Omega|$. The effective property, $\boldsymbol{IE}^{*}$, is the usual elasticity tensor for macrostructural analyses. Computationally intensive methods may be used to solve the loadings over the RVE (Zohdi and Wriggers [10]). However, it is often advantageous to seek faster approximation methods. *Such quick approximations accelerate initial design iteration to minimize time and experimental cost–the objective of this paper.* In this manuscript, we utilize the correlated phase-averaged micro- and macrostructural loadings to explore the distribution of expected responses for in the unique setting of mixed recycled material content in construction materials. We will focus on isotropic materials for both the particulate and the binder.

The objective is to provide designers with an easy-to-use framework that identifies the distribution of stress contributions from the micro- and macroscale based on mixed recycled content, in order to reduce product development time and costs.

The following sections define the modeling method and results. Section 3 provides the fundamental property estimates for particulate mixtures. Section 4 derives the formulae for estimating variable properties from a distribution of particle properties starting from the fundamental property estimate equations in Section 3. Section 5 applies the variable property estimates developed in Section 4 to the particle-matrix stress concentration relations developed by [11] to provide quick estimates in material development of mixed recycled waste and infrastructure materials.

3. Effective property estimates

Maxwell [12,13] and Lord Rayleigh [14] were some of the first to propose models to estimate the macroscopic properties of heterogeneous materials. An extremely important contribution came in the 1960s: Hashin–Shtrikman bounds (Hashin and Shtrikman [15,16], Hashin [17]). These bounds provide the tightest range where volumetric data and phase contrasts of the constituents are the only known parameters. Interphase boundaries are assumed to be well bonded. For bulk modulus, we write,

$$\kappa^{*,-} \stackrel{\text{def}}{=} \kappa_1 + \frac{v_2}{\frac{1}{\kappa_2-\kappa_1} + \frac{3(1-v_2)}{3\kappa_1+4\mu_1}} \leqslant \kappa^{*} \leqslant \kappa_2 + \frac{1-v_2}{\frac{1}{\kappa_1-\kappa_2} + \frac{3v_2}{3\kappa_2+4\mu_2}} \stackrel{\text{def}}{=} \kappa^{*,+}, \quad (1)$$

and for the shear modulus

$$\mu^{*,-} \stackrel{\text{def}}{=} \mu_1 + \frac{v_2}{\frac{1}{\mu_2-\mu_1} + \frac{6(1-v_2)(\kappa_1+2\mu_1)}{5\mu_1(3\kappa_1+4\mu_1)}} \leqslant \mu^{*} \leqslant \mu_2 + \frac{(1-v_2)}{\frac{1}{\mu_1-\mu_2} + \frac{6v_2(\kappa_2+2\mu_2)}{5\mu_2(3\kappa_2+4\mu_2)}} \stackrel{\text{def}}{=} \mu^{*,+}, \quad (2)$$

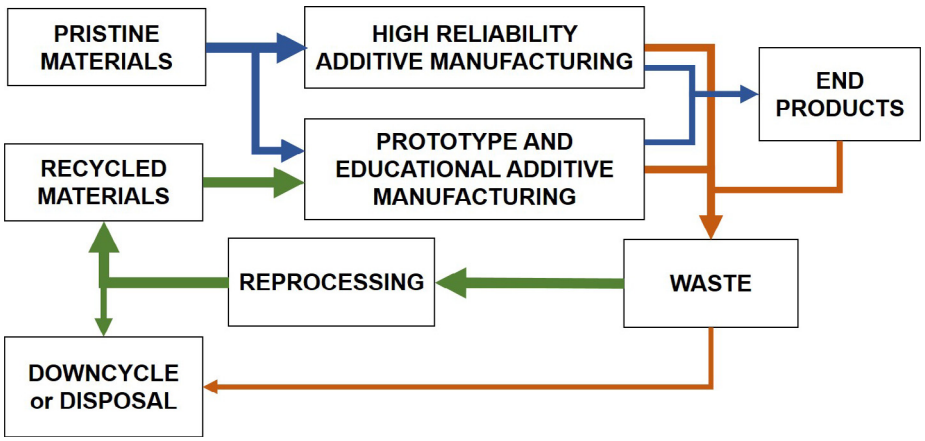

Fig. 2. Flowchart of material pathways for pristine and recycled materials in additive manufacturing.

where κ_2 and κ_1 are the bulk moduli and μ_2 and μ_1 are the shear moduli of the respective phases ($\kappa_2 \geqslant \kappa_1$ and $\mu_2 \geqslant \mu_1$), and where v_2 is the second phase volume fraction. Phase 2 is the stiffer of the two constituents (which usually corresponds to the particles). The effective properties are then estimated as a convex combination of the bounds, as follows,

$$\kappa^* \approx \phi\kappa^{*,+} + (1-\phi)\kappa^{*,-} \tag{3}$$

and

$$\mu^* \approx \phi\mu^{*,+} + (1-\phi)\mu^{*,-}, \tag{4}$$

where $0 \leqslant \phi \leqslant 1$ is a parameter such that when $\phi = 0$ we have the lower bound, $\phi = 1$ we have the upper bound and $\phi = 1/2$ we have the average of the bounds. When particles are well separated and spherical, ϕ is more accurately estimated closer to 0, as particles become flatter or interact (touch) more, ϕ, is more accurately estimated closer to 1. Typically, $\phi = 0.5$ initially and refine the selection with test data.[1]

Phase 1 may be modulated with a distribution as may be the case in mixed recycled material as the softer material between the matrix and the particles. This modulation alters only the value of the bounds, not the formulation. Numerical results are used as the analytical formulation involves an open question dating back to 1932 related to the work of Fieller [18]. Numerical distributional effects from variable input material properties on shear and bulk moduli are shown in Fig. 3, where the phase 1 bulk modulus (κ_1) is half the phase 2 bulk modulus (κ_2), the phase 2 shear modulus (μ_2) is.577 the phase 2 bulk modulus, the phase 1 shear modulus (μ_1) is.4 the phase 1 bulk modulus, and the standard deviation of both the shear and bulk moduli of phase 1 are 5% of their respective values. A boxplot is overlaid for each 10% change in volume fraction and simulation of 3000 samples. The whiskers of each box reach from the 2.5 percentile to the 97.5 percentile of κ^* and μ^* with ϕ set to 0.5, as is typical. Stresses are plotted as a ratio of the 'stiffer' material for easy reference in design.

The general theory of random heterogeneous media is well reviewed in Torquato [19]. Jikov et al. [20] provides a general interdisciplinary discussion. Mathematical formulations are provided by Hashin [17], Mura [21] or Markov [22]. Defect, porous, and cracked media is accounted by Kachanov [23], Kachanov, Tsukrov and Shafiro [24], Kachanov and Sevostianov [25], Sevostianov, Gorbatikh and Kachanov [26], Sevostianov and Kachanov [27]. For computational aspects for simulation and fine-tuned design iteration see Ghosh [28], Ghosh and Dimiduk [29] and Zohdi and Wriggers [10].

[1] **Note:** One may compute the effective Poisson ratio $v^* = \frac{3\kappa^* - 2\mu^*}{2(3\kappa^* + \mu^*)}$ and the effective Young's modulus $E^* = 2\mu^*(1+v^*) = 3\kappa^*(1-2v^*)$ from κ^* and μ^*.

4. Variable property distributions

Once the phase-averaged microstructural material properties have been formulated, we apply a distributional perturbation to the additive (particulate recycled material).

Beginning with Eq. (1) and reformulating with a random, normally distributed, variable for Phase 1 material properties ($\kappa_1 \to K, \mu_1 \to M$), where $K \sim N(\bar{\mu}_{\kappa_1}, s^2_{\kappa_1})$ and $M \sim N(\bar{\mu}_{\mu_1}, s^2_{\mu_1})$. For the lower bound, we write,

$$\kappa^{*,-} = K + \frac{v_2}{\frac{1}{\kappa_2 - K} + \frac{3(1-v_2)}{3K+4M}} \tag{5}$$

$$\kappa^{*,-} = K + \frac{K(3v_2\kappa_2) + MK(-4v_2) + K^2(-3v_2) + M(4v_2\kappa_2)}{M(4) + K(3v_2) + (3\kappa_2 - 3v_2\kappa_2)} \tag{6}$$

The solution then takes the generalized form, with resultant random variable, R as a function of the sum of K and a ratio of functions X_2 and X_3 in the variables K and M. The steps are outlined for the analytical approach; however, several terms appear that have no closed form for Gaussian distributed random variables.

The ratios and products of Gaussian distributed random variables have been examined in multiple fields with varying approaches. A closed form solution exists for the ratio zero mean independent variables and for correlated non-zero mean variables [30,31], and very recently for the product of correlated zero-mean Gaussian distributed random variables [32]. A closed form also exists for ratio of complex Gaussian distributed random variables [33]. Computational methods are often employed for other variations as well as products of correlated Gaussian distributed random variables [31].

$$R(K, X_2, X_3) = K + \frac{X_2(K,M)}{X_3(K,M)} \tag{7}$$

The cumulative distribution function (CDF) is defined as:

$$F_Z(z) = F(K, X_2, X_3 \leqslant r) = \iiint_{A_R} f_{K,X_2,X_3}(k, x_2, x_3)\,dk\,dx_2\,dx_3 \tag{8}$$

where CDF of the denominator, X_3, is of the form,

$$F_{X_3}(x_3) = \int_{A_{X_3}} f_{X_3}(x_3)\,dx_3 = \int_{A_{X_3}} f(3v_2K + 4M + 3v_2\kappa_2)\,dx_3 \tag{9}$$

thus X_3 is distributed normally as,

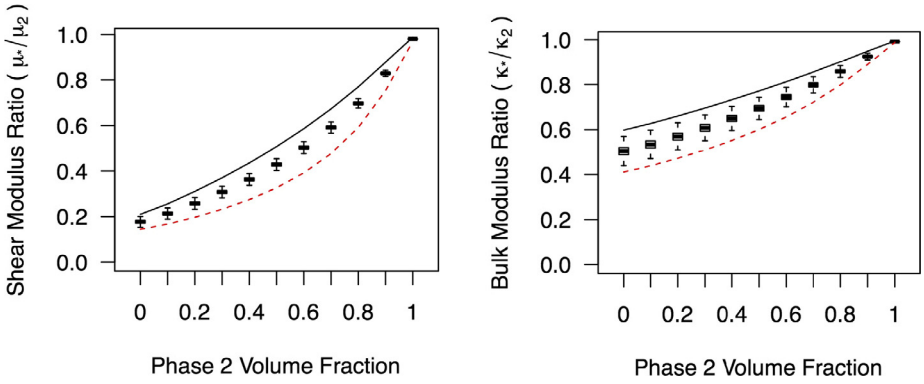

Fig. 3. Shear(left) and bulk (right) modulus bounds with variable lower modulus input materials properties with output normalized to the higher material modulus.

$$X_3 \sim \mathcal{N}\left(3v_2\bar{\mu}_{\kappa_1} + 4\bar{\mu}_{\mu_1} + (3\kappa_2 - 3v_2\kappa_2), 9v_2^2 s^2_{\kappa_1} + 16 s^2_{\mu_1}\right) \tag{10}$$

$$F_{X_2}(x_2) = \int_{A_{X_2}} f_{X_2}(w)dw \tag{11}$$

$$F_{X_2}(x_2) = \int_{A_{X_2}} (f(-3v_2K^2) + f(3v_2\kappa_2 K) + f(4v_2\kappa_2 M) - f(4v_2 KM))dx_2 \tag{12}$$

We can simplify the calculation analytically but simulate the resultant distribution due to the final term in $f(K,M)$. The product of two Gaussian distributed random variables is not strictly Gaussian. However, a sufficiently small ratio of standard deviation to mean the results approach Gaussian and may be approximated as such. We numerically compute the result and thus avoid any errors from a simplified model. A similar approach is then followed for each of the upper and lower bounds of bulk and shear modulus. For the upper bound on bulk modulus, we write,

$$\kappa^{*,+} = \kappa_2 + \frac{1 - v_2}{\frac{1}{K-\kappa_2} + \frac{3v_2}{3\kappa_2 + 4\mu_2}} \tag{13}$$

$$\kappa^{*,+} \sim \frac{\mathcal{N}(a_0 + a_1\bar{\mu}_{\kappa_1}, s^2_{\kappa_1} a_1^2)}{\mathcal{N}(b_0 + b_1\bar{\mu}_{\kappa_1}, s^2_{\kappa_1} b_1^2)} + \kappa_2 \tag{14}$$

where $a_0 = \kappa_2(1-v_2)(3\kappa_2 + 4\mu_2), a_1 = (1-v_2)(3\kappa_2 + 4\mu_2)$, $b_0 = 3\kappa_2 + 4\mu_2 - 3v_2\kappa_2$, and $b_1 = 3v_2$. For the upper bound of shear modulus we write,

$$\mu^{*,+} \sim \frac{\mathcal{N}(a_2 + a_3\bar{\mu}_{\mu_1}, s^2_{\mu_1} a_3^2)}{\mathcal{N}(b_2 + b_3\bar{\mu}_{\mu_1}, s^2_{\mu_1} b_3^2)} + \mu_2 = \frac{\mathcal{N}(\bar{\mu}_Y, s_Y^2)}{\mathcal{N}(\bar{\mu}_Z, s_Z^2)} + \mu_2 \tag{15}$$

$$\mu^{*,+} \sim \mathcal{M}(Y,Z) + \mu_2 \tag{16}$$

where $a_2 = (1-v_2)5\mu_2^2(3\kappa_2 + 4\mu_2), a_3 = (1-v_2)5\mu_2(3\kappa_2 + 4\mu_2), b_2 = 5\mu_2(1-v_2)3\kappa_2 + 4\mu_2 - 6v_2(\kappa_2 + 2\mu_2)$, and $b_3 = 6v_2(\kappa_2 + 2v_2), Y$ and Z are substitution variables to simplify the notation, w is a variable representing the ratio of $Y:Z$, and ρ is the correlation coefficient of Y and Z.

The distribution for a ratio of Gaussian distributed variables follows that of Marsaglia [31] and Hinkley [30] and adopts their notation for $L(\cdot)$.

$$\mathcal{M}(Y,Z) \stackrel{\text{def}}{=} \sim L\left(\frac{\bar{\mu}_Y - \bar{\mu}_Z w}{s_Y s_Z \alpha(w)}, \frac{-\bar{\mu}_Z}{s_Z}; \frac{s_Z w - \rho s_Y}{s_Y s_Z \alpha(w)}\right) + L\left(\frac{\bar{\mu}_Y - \bar{\mu}_Z w}{s_Y s_Z \alpha(w)}, \frac{\bar{\mu}_Z}{s_Z}; \frac{s_Z w - \rho s_Y}{s_Y s_Z \alpha(w)}\right) \tag{17}$$

$$\alpha(w) = \left(\frac{w^2}{s_Y^2} - \frac{2\rho w}{s_Y s_Z} + \frac{1}{s_Z^2}\right) \tag{18}$$

For the lower bound of shear modulus we write,

$$\mu^{*,-} = M + \frac{v_2}{\frac{1}{\mu_2 - M} + \frac{6(1-v_2)(K+2M)}{5M(3K+4M)}} \tag{19}$$

$$\mu^{*,-} = M + \frac{a_4 KM + a_5 KM^2 + a_6 M^2 + a_7 M^3}{b_4 K + b_5 KM + b_6 M + b_7 M^2} \tag{20}$$

where $a_4 = 15v_2\mu_2, a_5 = -15v_2, a_6 = 20v_2\mu_2, a_7 = -20v_2, b_4 = (1-v_2)6\mu_2, b_5 = 9 + 6v_2, b_6 = (1-v_2)12\mu_2$, and $b_7 = 8 + 12v_2$. Due to the random variable products and ratios this relation does not reduce to a closed form distribution and is numerically computed.

Modulating phase 2 provides similar mathematical forms. For shear modulus, we write,

$$\mu^{*,-} \sim \frac{\mathcal{N}(a_8 + a_9\bar{\mu}_{\mu_2}, a_9^2 s^2_{\mu_2})}{\mathcal{N}(b_8 + b_9\bar{\mu}_{\mu_2}, b_9^2 s^2_{\mu_2})} + \mu_1 = \frac{\mathcal{N}(\bar{\mu}_{Y_2}, s^2_{Y_2})}{\mathcal{N}(\bar{\mu}_{Z_2}, s^2_{Z_2})} + \mu_1 \tag{21}$$

$$\mu^{*,-} \sim \mathcal{M}(Y_2, Z_2) + \mu_1 \tag{22}$$

where $a_8 = 5\mu_1(3\kappa_1 + 4\mu_1), a_9 = -5\mu_1^2 v_2(3\kappa_1 + 4\mu_1), b_8 = (1-v_2)6(\kappa_1 + 2\mu_1)$, and $b_9 = 15\kappa_1\mu_1 + 20\mu_1^2 + 6(1-v_2)(\kappa_1\mu_1 + 2\mu_1^2)$.

$$\mu^{*,+} = M + \frac{(1 - v_2)}{\frac{1}{\mu_1 - M} + \frac{6v_2(K+2M)}{5M(3K+4M)}} \tag{23}$$

$$\mu^{*,+} = M + \frac{a_{10} KM + a_{11} KM^2 + a_{12} M^2 + a_{13} M^3}{b_{10} K + b_{11} KM + b_{12} M + b_{13} M^2} \tag{24}$$

where $a_{10} = 15\mu_1(1-v_2), a_{11} = 15(v_2 - 1), a_{12} = 20\mu_1(1-v_2), a_{13} = 20(v_2 - 1), b_{10} = 6v_2, b_{11} = 15, b_{12} = 12v_2$, and $b_{13} = 20$.

For bulk modulus, we write,

$$\kappa^{*,+} = K + \frac{1 - v_2}{\frac{1}{\kappa_1 - K} + \frac{3v_2}{3K+4M}} \tag{25}$$

$$\kappa^{*,+} = K + \frac{a_{14} K + a_{15} K^2 + a_{16} KM + a_{17} M}{b_{14} K + b_{15} M + b_{16}} \tag{26}$$

where $a_{14} = 3\kappa_1 - 3\kappa_1 v_2, a_{15} = 3v_2 - 3, a_{16} = 4\kappa_1 - 4\kappa_1 v_2, a_{17} = 4v_2 - 4$, $b_{14} = 3 - 3v2, b_{15} = 4$, and $b_{16} = 3v_2$.

$$\kappa^{*,-} = \kappa_1 + \frac{v_2}{\frac{1}{K - \kappa_1} + \frac{3(1-v_2)}{3\kappa_1 + 4\mu_1}} \tag{27}$$

$$\kappa^{*,-} = \kappa_1 + \frac{K(v_2 3\kappa_1 + v_2 4\mu_1) - 3v_2\kappa_1^2 - 4v_2\kappa_1\mu_1}{K(3 - 3v_2) + 3v_2\kappa_1 4\mu_1} \tag{28}$$

$$\kappa^{*,-} \sim \frac{\mathcal{N}(a_{18} + a_{19}\bar{\mu}_{\kappa_2}, a_{19}^2 s^2_{\kappa_2})}{\mathcal{N}(b_{17} + b_{18}\bar{\mu}_{\kappa_2}, b_{18}^2 s^2_{\kappa_2})} + \kappa_1 = \frac{\mathcal{N}(\bar{\mu}_{Y_3}, s^2_{Y_3})}{\mathcal{N}(\bar{\mu}_{Z_3}, s^2_{Z_3})} + \kappa_1 \tag{29}$$

$$\kappa^{*,-} \sim \mathcal{M}(Y_3, Z_3) + \mu_1 \tag{30}$$

where $a_{18} = -3v_2\kappa_1^2 - 4v_2\kappa_1\mu_1, a_{19} = v_2 3\kappa_1 + v_2 4\mu_1, b_{17} = 3v_2\kappa_1 4\mu_1$, $b_{18} = 3 - 3v_2$,

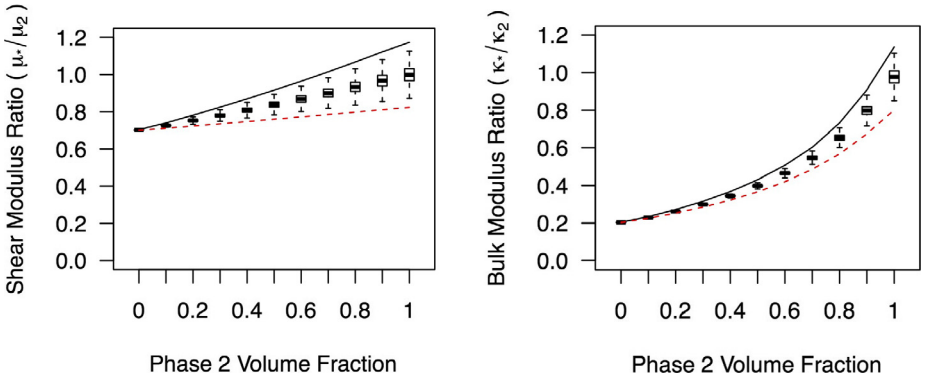

Fig. 4. Shear(left) and bulk (right) modulus bounds with variable upper modulus input materials properties with output normalized to the expected value of the higher material modulus.

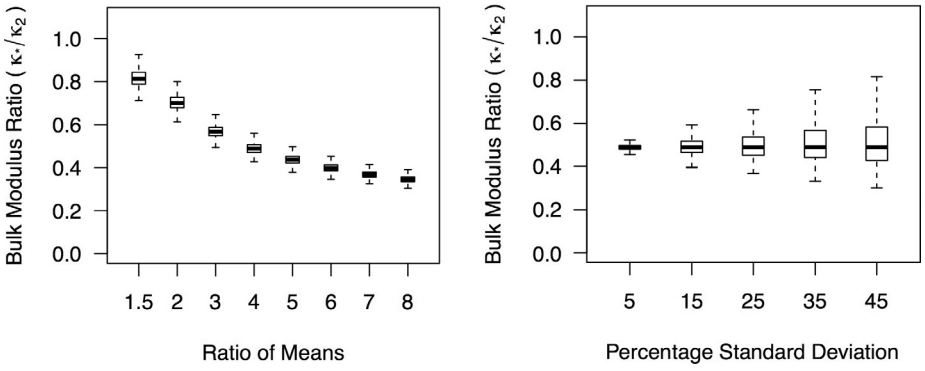

Fig. 5. Estimation changes as bulk modulus ratio increases with fixed 10% standard deviation (left); estimation changes as the variance of phase 2 bulk modulus increases, with fixed bulk modulus ratio (right).

Phase 2 may be modulated with a distribution as may be the case in some mixed recycled material constituents with softer construction materials. This modulation alters only the value of the bounds, not the formulation. Numerical results are used as the analytical formulation involves non-closed form interactions of random variables. Numerical distributional effects from variable input material properties on shear and bulk moduli are shown in Fig. 4, where the phase 1 bulk modulus (κ_1) is 20% the phase 2 bulk modulus (κ_2), the phase 2 shear modulus (μ_2) is.5 the phase 2 bulk modulus, the phase 1 shear modulus μ_1) is.4 the phase 1 bulk modulus, and the standard deviation of both the shear and bulk moduli of phase 1 are 5% of their respective values. A boxplot is overlaid for each 10% change in volume fraction. The whiskers of each box reach from the 2.5 percentile to the 97.5 percentile of κ^* and μ^* with ϕ set to 0.5, as is typical. Stresses are plotted as a ratio of the 'stiffer' material for easy reference in design.

As may often be the case with mixed recycled plastics, the material properties may vary in two ways. First, the difference in modulus between the matrix binder and the particulate may be larger or smaller. Second, the variance of the particulate (recycled plastic) material properties may be larger or smaller. These potential variations are computed for bulk modulus with the fixed volume fraction of 50% and estimated ϕ of 0.5. For a fixed standard deviation in bulk modulus and ϕ, but an increasing ratio of phase 2 mean bulk modulus to phase 1, the estimated κ^* trends away from the global maximum (Fig. 5 (left)). As the selection of stiffer material becomes much stiffer, the impact of variation in the softer material plays a less significant role than the difference in mean material properties, When the variance of phase 1 bulk modulus increases as a percentage of the mean value, the spread of potential κ^* values similarly deviates (Fig. 5 (right)).

5. Particle-matrix load sharing

Load-sharing between the binder and particulate at the microstructural scale are computed by decomposing the average stress over Ω into an average over each phase as in Zohdi [11]:

$$\langle \boldsymbol{\sigma} \rangle_{\Omega} = \frac{1}{|\Omega|}\left(\int_{\Omega_1} \boldsymbol{\sigma}\, d\Omega + \int_{\Omega_2} \boldsymbol{\sigma}\, d\Omega \right) = v_1 \langle \boldsymbol{\sigma} \rangle_{\Omega_1} + v_2 \langle \boldsymbol{\sigma} \rangle_{\Omega_2}, \tag{31}$$

where Ω_1 and Ω_2 denote phase 1 and phase 2, respectively. Phase 1 is usually the binder and phase 2 is usually the particulate additive. The resulting decomposition for the stresses is:

$$\langle \boldsymbol{\sigma} \rangle_{\Omega} = v_1 \langle \boldsymbol{\sigma} \rangle_{\Omega_1} + v_2 \langle \boldsymbol{\sigma} \rangle_{\Omega_2} = \left(\boldsymbol{I}\boldsymbol{I}_1 + v_2 (\boldsymbol{I}\boldsymbol{I}_2 - \boldsymbol{I}\boldsymbol{I}_1) : \boldsymbol{C}^{\epsilon,2} \right) : \langle \epsilon \rangle_{\Omega}, \tag{32}$$

where

$$\boldsymbol{C}^{\epsilon,2} \stackrel{\text{def}}{=} \left(\frac{1}{v_2} (\boldsymbol{I}\boldsymbol{I}_2 - \boldsymbol{I}\boldsymbol{I}_1)^{-1} : (\boldsymbol{I}\boldsymbol{I}^* - \boldsymbol{I}\boldsymbol{I}_1) \right) \tag{33}$$

is called the strain concentration function, with $\boldsymbol{C}^{\epsilon,2} : \langle \boldsymbol{\epsilon} \rangle_{\Omega} = \langle \boldsymbol{\epsilon} \rangle_{\Omega_2}$. The strain concentration tensor $\boldsymbol{C}^{\epsilon,2}$ relates the average strain over the particle phase (2) to the average strain over all phases. Similarly, for the variation in the stress we have $\boldsymbol{C}^{\epsilon,2} : \boldsymbol{I}\boldsymbol{E}^{*-1} : \langle \boldsymbol{\sigma} \rangle_{\Omega} = \boldsymbol{I}\boldsymbol{E}_2^{-1} : \langle \boldsymbol{\sigma} \rangle_{\Omega_2}$, which reduces to $\boldsymbol{I}\boldsymbol{E}_2 : \boldsymbol{C}^{\epsilon,2} : \boldsymbol{I}\boldsymbol{E}^{*-1} : \langle \boldsymbol{\sigma} \rangle_{\Omega} \stackrel{\text{def}}{=} \boldsymbol{C}^{\sigma,2} : \langle \boldsymbol{\sigma} \rangle_{\Omega} = \langle \boldsymbol{\sigma} \rangle_{\Omega_2}$. $\boldsymbol{C}^{\sigma,2}$ is known as the stress concentration tensor and it relates the average stress in the particle phase to that in the whole RVE. In the case of isotropy we may write:

$$C_{\kappa}^{\sigma,2} \stackrel{\text{def}}{=} \frac{1}{v_2} \frac{\kappa_2}{\kappa^*} \frac{\kappa^* - \kappa_1}{\kappa_2 - \kappa_1} \quad \text{and} \quad C_{\mu}^{\sigma,2} \stackrel{\text{def}}{=} \frac{1}{v_2} \frac{\mu_2}{\mu^*} \frac{\mu^* - \mu_1}{\mu_2 - \mu_1} \tag{34}$$

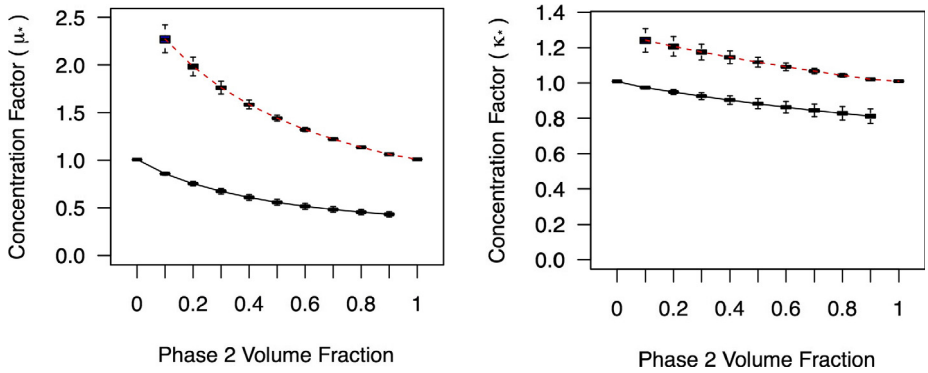

Fig. 6. Shear (left) and bulk (right) stress concentration factor bounds with variable lower modulus input materials properties. Stress concentration tends towards neutral for the material with a larger volume fraction.

where $C_{\kappa}^{\sigma,2}\langle \frac{tr\boldsymbol{\sigma}}{3}\rangle_{\Omega} = \langle \frac{tr\boldsymbol{\sigma}}{3}\rangle_{\Omega_2}$ and where $C_{\mu}^{\sigma,2}\langle \boldsymbol{\sigma}'\rangle_{\Omega} = \langle \boldsymbol{\sigma}'\rangle_{\Omega_2}$. Stress concentrations are not expected in a homogeneous material, thus $C_{\kappa}^{\sigma,2} = C_{\mu}^{\sigma,2} = 1$, which matches expectations. For the binder material (with isotropy), we write,

$$C_{\kappa}^{\sigma,1} \overset{\text{def}}{=} \frac{1}{v_1}(1 - v_2 C_{\kappa}^{\sigma,2}) \qquad \text{and} \qquad C_{\mu}^{\sigma,1} \overset{\text{def}}{=} \frac{1}{v_1}(1 - v_2 C_{\mu}^{\sigma,2}). \tag{35}$$

The fraction of total stress carried by each phase may then be determined using Eq. (31).

Following the decomposition of stress concentration factors, the variation in properties of either phase contributes to similar results. When the volume of phase 2 is low, the variation in stress concentration is larger and converges as the volume fraction increases. This trend is visible for both bulk (κ^*) and shear (μ^*) modulus concentration factors (Fig. 6).

6. Summary & extensions

This work promotes a reduction in waste generation, plastic production, and construction material consumption, as well as increased adoption of particle-enhanced materials in consumer and industrial applications. We expanded previous work on correlating phase-averaged microstructural stresses to the macrostructural loading to include variational material properties. This expansion provides a wide range of applicability in material and product development. This novel framework and easy-to-use design tool identifies and indicates variational trends from recycled material-enhanced composites, which should reduce product development time and cost.

Beyond construction materials, the approach developed here may also be useful where processes have a distribution of materials and rapid design iteration is desired. Examples of such new composite material manufacturing techniques are multiphase extrusion (Khalifa et al. [34]), inter-laminar glass reinforcement (Bian et al. [35]), selective laser sintering (Gu et al. [36]), sacrificial patterning (Singh and Singh [37]), electric field assistance (Decker and Gan [38]), microcutting arrays (Pacella et al. [39]), and reinforcement with carbon nanotubes (Isaza et al. [40]). Regardless of the use, this methodology serves to promote a more circular economy by accelerating design of materials which utilized mixed recycled waste.

The quantity, ϕ, is a function of the microstructure and needs to be calibrated. For stiff spherical particles, at low volume fractions, for example under 15%, as is the case with current experimental plastic impregnated concrete, where the particles are not generally in contact, the lower bound is more accurate. Thus, one would pick $\phi \leqslant 0.5$ to bias the estimate to the lower bound for the design of these materials. However, given the same volume fraction and flatter particles that interact (touch), then the upper bound is likely to be more accurate. Thus, one would pick $\phi \geqslant 0.5$. For 3-D printed waste, the usual form is flat flakes and would bias new construction materials toward a greater value of ϕ. One can calibrate ϕ by comparing it to different experiments (see, for example, Zohdi et al. [41]). This methodology may also be used to quickly estimate the multiphase extension of the Hashin–Shtrikman bounds (Hashin and Shtrikman [16]) by grouping materials into a distribution of properties. Once initial screening of material mixtures is complete using the methodology in this paper, complex geometries with variable material properties become of interest. This specific extension is well suited for investigation using the Finite Element Method. This is currently being pursued by the authors.

Acknowledgements

This research did not receive any specific grant from funding agencies in the public, commercial, or not-for-profit sectors.

References

[1] K.A. O'Connell, California Adopts Zero Waste Goal in Strategic Plan (Apr. 2002). http://www.waste360.com/mag/wastecaliforniaadoptszero.
[2] M. Vilella, Zero Waste Cities: At The Forefront Of The Sustainable Development Goals Agenda (Sep. 2016).https://www.huffingtonpost.com/mariel-vilella/zero-waste-cities-at-theb12029704.html.
[3] U. of Oregon, U of O Zero Waste Program (2012). http://zerowaste.uoregon.edu/.
[4] Waste Policies & Best Practice.https://www.zerowasteeurope.eu/waste/.
[5] B. Messenger, 90 NGOs Launch Plastic Waste Reduction & Marine Pollution Initiative, Waste Management WorldInternational Solid Waste Association Vienna, Austria.https://waste-management-world.com/a/90-ngos-launch-plastic-waste-reduction-marine-pollution-initiative.
[6] R.L. Taylor, S.B. Villas-Boas, Bans vs. Fees: Disposable Carryout Bag Policies and Bag Usage, Applied Economic Perspectives and Policy 38(2), 2016, pp. 351–372. doi: https://doi.org/10.1093/aepp/ppv025. https://academic.oup.com/aepp/article/38/2/351/1739749.
[7] F.P. La Mantia, Polymer mechanical recycling: downcycling or upcycling?, Progr Rubber Plast. Recycl. Technol. 20 (1) (2004) 11–24.
[8] A.K. Jassim, Recycling of polyethylene waste to produce plastic cement, Proc. Manufact. 8 (2017) 635–642, https://doi.org/10.1016/j.promfg.2017.02.081. http://linkinghub.elsevier.com/retrieve/pii/S2351978917300872.
[9] R. Siddique, J. Khatib, I. Kaur, Use of recycled plastic in concrete: a review, Waste Manage. 28 (10) (2008) 1835–1852, https://doi.org/10.1016/j.wasman.2007.09.011. http://linkinghub.elsevier.com/retrieve/pii/S0956053X07003054.
[10] T.I. Zohdi, P. Wriggers, first ed., Introduction Computational Micromechics, Vol. 20, Springer-Verlag, Berlin, Heidelberg, 2005. http://www.springer.com/us/book/9783540774822.
[11] T. Zohdi, An explicit macro-micro phase-averaged stress correlation for particle-enhanced composite materials in loaded structures, Int. J. Eng. Sci. 109 (2016) 1–13, https://doi.org/10.1016/j.ijengsci.2016.09.005. http://linkinghub.elsevier.com/retrieve/pii/S0020722516307571.
[12] J.C. Maxwell, On the dynamical theory of gases, Philos. Trans. R. Soc. Lond. 157 (1867) 49–88. http://www.jstor.org/stable/108968.

[13] J.C. Maxwell, A Treatise on Electricity and Magnetism, Claredon Press, Oxford, 1873. https://www.loc.gov/item/03015568/.
[14] J. Rayleigh, On the influence of obstacles arranged in rectangular order upon the properties of a medium, London Edinburgh Dublin Philos. Mag. J. Sci. 34 (211) (1892) 481–502, https://doi.org/10.1080/14786449208620364.
[15] Z. Hashin, S. Shtrikman, On some variational principles in anisotropic and nonhomogeneous elasticity, J. Mech. Phys. Solids 10 (4) (1962) 335–342, https://doi.org/10.1016/0022-5096(62)90004-2. http://www.sciencedirect.com/science/article/pii/0022509662900042.
[16] Z. Hashin, S. Shtrikman, A variational approach to the theory of the elastic behaviour of multiphase materials, J. Mech. Phys. Solids 11 (2) (1963) 127–140, https://doi.org/10.1016/0022-5096(63)90060-7. http://www.sciencedirect.com/science/article/pii/0022509663900607.
[17] Z. Hashin, Analysis of composite materials a survey, J. Appl. Mech. 50 (3) (1983) 481–505, https://doi.org/10.1115/1.3167081.
[18] E.C. Fieller, The distribution of the index in a normal bivariate population, Biometrika 24 (3–4) (1932) 428–440, https://doi.org/10.1093/biomet/24.3-4.428. https://academic.oup.com/biomet/article/24/3-4/428/378900.
[19] S. Torquato, first ed., Random Heterogeneous Materials – Microstructure and Macroscopic Properties, Vol. 16, Springer-Verlag, New York, 2002. www.springer.com/gp/book/9780387951676.
[20] V. Jikov, S. Kozlov, O. Oleinik, Homogenization of Differential Operators and Integral Functionals — V.V. Jikov — Springer, 1st Edition., Springer-Verlag, 1994. http://www.springer.com/gp/book/9783642846618.
[21] T. Mura, second ed., Micromechanics of Defects in Solids, Vol. 3, Springer, Netherlands, 1987. http://www.springer.com/gp/book/9789024732562.
[22] , first ed.K. Markov, L. Preziosi (Eds.), Heterogeneous Media - Micromechanics Modeling Methods and Simulations, Birkhuser Basel, 2000. http://www.springer.com/gp/book/9780817640835.
[23] M. Kachanov, Elastic Solids with Many Cracks and Related Problems, in: J.W. Hutchinson, T.Y. Wu (Eds.), Advances in Applied Mechanics, Vol. 30, Elsevier, 1993, pp. 259–445. http://www.sciencedirect.com/science/article/pii/S0065215608701765.
[24] M. Kachanov, I. Tsukrov, B. Shafiro, Effective moduli of solids with cavities of various shapes, Appl. Mech. Rev. 47 (1S) (1994) S151–S174, https://doi.org/10.1115/1.3122810.
[25] M. Kachanov, I. Sevostianov, On quantitative characterization of microstructures and effective properties, Int. J. Solids Struct. 42 (2) (2005) 309–336, https://doi.org/10.1016/j.ijsolstr.2004.06.016. http://linkinghub.elsevier.com/retrieve/pii/S0020768304003324.
[26] I. Sevostianov, L. Gorbatikh, M. Kachanov, Recovery of information on the microstructure of porous/microcracked materials from the effective elastic/conductive properties, Mater. Sci. Eng. A 318 (1) (2001) 1–14.
[27] I. Sevostianov, M. Kachanov, Connections between elastic and conductive properties of heterogeneous materials, Adv. Appl. Mech., Vol. 42, Elsevier, 2009, pp. 69–252. http://linkinghub.elsevier.com/retrieve/pii/S0065215608000021.
[28] S. Ghosh, D. Dimiduk, Computational Methods for Microstructure-Property Relationships, first ed., Springer, US, 2011. http://www.springer.com/gp/book/9781441906427.
[29] S. Ghosh, Micromechanical Analysis and Multi-Scale Modeling Using the Voronoi Cell Finite Element Method, CRC Press/Taylor & Francis (2011), https://doi.org/10.1201/b10903.
[30] D.V. Hinkley, On the ratio of two correlated normal random variables, Biometrika 56 (3) (1969) 635–639.
[31] G. Marsaglia, Ratios of normal variables and ratios of sums of uniform variables, J. Am. Stat. Assoc. 60 (309) (1965) 193–204.
[32] S. Nadarajah, T.K. Pogny, On the distribution of the product of correlated normal random variables, C.R. Math. 354 (2) (2016) 201–204, https://doi.org/10.1016/j.crma.2015.10.019. http://linkinghub.elsevier.com/retrieve/pii/S1631073X15002873.
[33] R.J. Baxley, B.T. Walkenhorst, G. Acosta-Marum, Complex Gaussian ratio distribution with applications for error rate calculation in fading channels with imperfect CSI, Global Telecommunications Conference (GLOBECOM 2010), 2010 IEEE, IEEE, 2010, pp. 1–5. http://ieeexplore.ieee.org/abstract/document/5683407/.
[34] N.B. Khalifa, A. Foydl, D. Pietzka, A. Joger, Process limits of extrusion of multimaterial components, J. Manuf. Sci. Eng. 137 (5) (2015), https://doi.org/10.1115/1.4031091. 051001–051001–9.
[35] D. Bian, G. Satoh, Y.L. Yao, The laser interlaminar reinforcement of continuous glass fiber composites, J. Manuf. Sci. Eng. 137 (6) (2015) 061001.
[36] D. Gu, F. Chang, D. Dai, Selective laser melting additive manufacturing of novel aluminum based composites with multiple reinforcing phases, J. Manuf. Sci. Eng. 137 (2) (2015), https://doi.org/10.1115/1.4028925. 021010–021010–11.
[37] S. Singh, R. Singh, Study on tribological properties of AlAl2o3 composites prepared through FDMAIC route using reinforced sacrificial patterns, J. Manuf. Sci. Eng. 138 (2) (2015), https://doi.org/10.1115/1.4030772. 021009–021009–10.
[38] B.Y. Decker, Y.X. Gan, Electric field-assisted additive manufacturing polyaniline based composites for thermoelectric energy conversion, J. Manuf. Sci. Eng. 137 (2) (2015), https://doi.org/10.1115/1.4029398. 024504–024504–3.
[39] M. Pacella, D.A. Axinte, P.W. Butler-Smith, P. Shipway, M. Daine, C. Wort, An assessment of the wear characteristics of microcutting arrays produced from polycrystalline diamond and cubic boron nitride composites, J. Manuf. Sci. Eng. 138 (2) (2015), https://doi.org/10.1115/1.4030761. 021001–021001–16.
[40] C. Isaza, G. Sierra, J.M. Meza, A novel technique for production of metal matrix composites reinforced with carbon nanotubes, J. Manuf. Sci. Eng. 138 (2) (2015), https://doi.org/10.1115/1.4030377. 024501–024501–5.
[41] T.I. Zohdi, P. Monteiro, V. Lamour, Extraction of elastic moduli from granular compacts, Int. J. Fract. 115 (L49–L54).http://cmmrl.berkeley.edu/zohdipaper/30.pdf.